

## ARTICLE

# High Resolution Crossed Beams Scattering Study of the $F+HD\rightarrow DF+H$ Reaction<sup>†</sup>

Xing-an Wang<sup>a</sup>, Li Che<sup>a</sup>, Ze-feng Ren<sup>a</sup>, Ming-hui Qiu<sup>a,b</sup>, Dong-xu Dai<sup>a</sup>, Xiu-yan Wang<sup>a</sup>, Xue-ming Yang<sup>a\*</sup>

*a. State key Laboratory of Molecular Reaction Dynamics, Dalian Institute of Chemical Physics, Chinese Academy of Sciences, Dalian 116023, China*

*b. Department of Physics, Dalian Jiaotong University, Dalian 116028, China*

(Dated: Accepted on December 6, 2009)

Crossed beams scattering study was carried out on the  $F+HD\rightarrow DF+H$  reaction using high-resolution H-atom Rydberg tagging time-of-flight technique. Vibrational state-resolved differential cross sections were measured, with partial rotational state resolution, at eight collision energies in the range of 2.51–5.60 kJ/mol. Experimental results indicated that the product angular distributions are predominantly backward scattered. As the collision energy increases, the backward scattered peak becomes broader gradually. Dependence of product vibration branching ratios on the collision energy was also determined. The experimental results show that the DF products are highly inverted in the vibrational state distribution and the DF ( $v'=3$ ) product is the most populated state. Furthermore, the DF ( $v'=1$ ) product has also been observed at collision energy above 3.97 kJ/mol.

**Key words:**  $F+HD\rightarrow DF+H$ , Crossed beam, Rydberg tagging, Backward scattering

## I. INTRODUCTION

The  $F+HD$  reaction has played an important role in the study of reaction dynamics of elementary chemical reactions. This important reaction has also served as a textbook example of elementary chemical reactions. In the middle of 1980s, Lee and co-workers carried out a landmark crossed beams experiment on both reaction channels of the  $F+HD$  reaction:  $F+HD\rightarrow HF+D$  and  $F+HD\rightarrow DF+H$  [1]. Vibrational resolved differential cross sections (DCSs) were measured for the first time for this important reaction. In the  $F+HD\rightarrow HF+D$  channel, a clear forward scattering peak for the HF ( $v'=3$ ) product was observed, and was attributed to reaction resonances. Since then, significant efforts have been devoted to investigating the kinetics and dynamics of this reaction experimentally [2–8]. Extensive theoretical studies were also carried out on this reaction both in quantum dynamical calculations (QM) [2,3,9–15] and in quasiclassical trajectory (QCT) calculations [16,17]. In 2000, Liu and co-workers performed a crossed beams scattering study of the  $F+HD\rightarrow HF+D$  channel and observed an intriguing step-like structure in the excitation function [2]. This step-like structure was assigned to a reaction resonance of this system. Liu and coworkers also carried out a detailed study of the

$F+HD\rightarrow DF+H$  channel and measured the vibrational branching ratios for the  $DF+H$  product channel [4]. In a more recent follow-up study, Liu and co-workers [6] reported the state-to-state DCS at four collision energies in the range from 4.93 kJ/mol to 16.72 kJ/mol. Their results indicated that the product angular distributions are predominantly backscattered at low energies and shift toward sideways at higher energies, which is consistent with the earlier study by Lee and co-workers [1]. So far, all previous experimental DCSs on the  $F+HD\rightarrow DF+H$  reaction were acquired at collision energies higher than 4.93 kJ/mol.

In 2007, Yang, Zhang and co-workers carried out a combined experimental and theoretical study on the resonance-mediated  $F+HD\rightarrow HF+D$  reaction at the full quantum state resolved level [8]. The fast changing dynamics at the low collision energies obtained in this work provided an extremely accurate testing ground for the resonance picture of this benchmark system. An accurate resonance potential has also been obtained in this work. Up to now the  $F+HD\rightarrow DF+H$  channel, however, has not been studied using the high resolution H-atom Rydberg tagging technique.

In this paper, we report the results of our recent experimental study on the  $F+HD\rightarrow DF+H$  reactive channel in the collision energy range of 2.51–5.60 kJ/mol using the high resolution H-atom Rydberg tagging technique. This work is an extension of the series of works on the  $F+H_2/HD/D_2$  system [8,18–23] carried in our laboratory. Product vibrational state resolved DCSs with partial rotational state resolution were obtained in the collision energy range of 2.51–5.60 kJ/mol. Prod-

<sup>†</sup>Part of the special issue for “the Chinese Chemical Society’s 11th National Chemical Dynamics Symposium”.

\*Author to whom correspondence should be addressed. E-mail: xmyang@dicp.ac.cn

uct vibrational state distributions as well as rotational state distributions are determined in this work. The collision energy dependent product vibrational branching ratios are also reported.

## II. EXPERIMENTS

The experiments in the current work were carried out using the H-atom Rydberg “tagging” time-of-flight (HRTOF) technique [24,25]. Since this method has been described in detail in numerous previous papers, only a brief description is given here [24,25,27]. The key element of this technique is the excitation of the H-atom product to the high Rydberg states. The H products from the reaction were excited to a high Rydberg state using a two-step excitation scheme: VUV laser excitation at the Lyman- $\alpha$  wavelength (121.6 nm) from  $n=1$  to  $n=2$ , followed by a UV laser excitation from  $n=2$  to  $n\approx 45$  at the wavelength of about 365 nm. The VUV radiation at the Lyman- $\alpha$  wavelength is generated by difference frequency four-wave mixing ( $2\omega_1-\omega_2$ ) of 212.5 nm light and 845 nm light in a cell filled with a 3:1 ratio Ar-Kr mixture. Laser light at 212.5 nm was produced by doubling a 425 nm dye laser (Sirah, PESC-G-24), pumped by the third harmonic output of a Nd:YAG laser (Spectra Physics Pro-290). Laser radiation at 845 nm used here was the direct output of a dye laser (Continuum ND6000), pumped by a portion of the 532 nm output of the YAG laser. These laser beams were then focused into the Kr/Ar mixing gas cell where the four wave mixing VUV radiation was generated. The remaining 532 nm light from the YAG laser was used to pump a third dye laser (Sirah, PESC-G-24), operating about 730 nm, the output from which the frequency is doubled to about 365 nm, and used to excite the H atom from the  $n=2$  level to a high Rydberg state with  $n\approx 45$ , which is slightly below the ionization threshold. The charged species formed at the tagging region by the lasers were extracted away by a small electric field (about 30 V/cm) placed across the interaction region. The neutral Rydberg tagged H-atoms then fly a certain distance and reach a multichannel plate (MCP) detector with a fine grid (grounded) in the front. After passing through the grid, the Rydberg H-atoms are then immediately field-ionized by the electric field applied between the front plate of the Z-stack MCP detector and the fine metal grid. The signal received by the MCP is then amplified by a fast preamplifier and counted by a multichannel scaler (MCS).

In this experiment, the F-atom beam was generated by double stage pulsed discharge [26] of  $F_2$  (seeded in helium, mixing ratio about 5%, total pressure about 556 kPa). After passing two skimmers (orifice 1.5 and 2 mm), the F atom beam was crossed with the other skimmed (orifice 1.5 mm) pulsed molecular beam of HD which was cooled by liquid nitrogen. The velocity of the F-atom beam is about 1.85 km/s with a speed ra-

tio of about 12. The velocity of the HD beam is about 1.25 km/s with a speed ratio of about 25. Nearly all of the HD molecules were populated on the ( $v=0, j=0$ ) state in the beam. The rotatable F-atom beam source [27] allows us to study the reaction at different collision energies, and we can determine the collision energy exactly due to the high speed ratios of both the F-atom beam and the HD beam. The product angular distribution was measured by taking the TOF spectra at different laboratory angles back and forth many times in order to reduce the systematic errors of the experimental data.

## III. RESULTS AND DISCUSSION

### A. Experimental time-of-flight spectra

The time-of-flight (TOF) spectra of the H-atom products of the F+HD reaction were measured using the HRTOF technique. TOF spectra were measured in every  $10^\circ$  in order to determine the full scattering picture of the reaction. The HD-beam is defined at  $0^\circ$  while the F-atom beam is rotatable. The collision energies varied from 4.93 kJ/mol to 5.60 kJ/mol by changing the crossing angle of the two beams.

Figure 1 shows the TOF spectra of the H atom products from the F-atom reaction with HD at two laboratory angles at the collision energies of 3.97 and

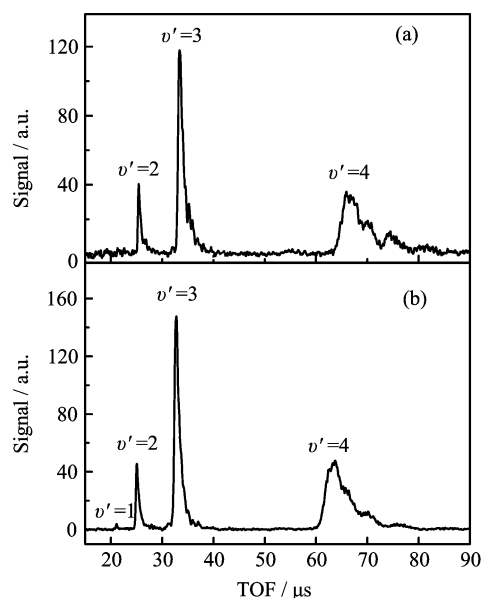


FIG. 1 TOF spectra of the H atom product from the F+HD $\rightarrow$ DF+H reaction: (a) detected angle in the laboratory coordinate  $\theta_L=110^\circ$ , 3.97 kJ/mol, (b)  $\theta_L=105^\circ$ , 4.26 kJ/mol, the two laboratory angles correspond roughly to the H-atom products scattered in the backward direction in the center-of-mass frame, relative to the HD beam direction at both collision energies.

4.26 kJ/mol. The two laboratory angles correspond roughly to the H-atom products scattered in the backward direction in the center-of-mass frame relative to the HD beam direction at both collision energies. Three sharp structures are observed at 3.97 kJ/mol. According to the energy conservation law, the three structures can be clearly assigned to the DF product in the  $v'=2$ , 3, 4 vibrational states. Rotational state peaks are partially resolved on the DF ( $v'=3$  and  $v'=2$ ) vibrational peaks. In contrast with the F+HD→HF+D channel, the rotational temperature is considerably colder in the DF+H channel. This large difference is obviously due to the fact that the two channels experiences very different transition state dynamics. While the HF+D channel occurs via a resonance mechanism, the DF+H channel goes through a direct abstraction mechanism. A small peak of the product DF ( $v'=1$ ) vibrational state was also observed at the collision energy of 4.26 kJ/mol or above. No signals from the DF ( $v'=0$ ) state were seen in the collision energies range we studied.

### B. State-resolved differential cross sections

The main structures in the TOF spectra can be easily assigned to the DF ro-vibrational states from the ground state  $F(^2P_{3/2})$  react with HD ( $v=0, j=0$ ). These TOF spectra were then converted to the CM frame with a standard Jacobian transformation to obtain product kinetic energy (KE) distributions. The product KE distributions at a specific scattering angle in the laboratory frame were simulated using a computer simulation program by adjusting the relative populations of the ro-vibrational states of the DF product. From the simulations, ro-vibrational state resolved differential cross sections (DCSs) were determined. By integrating the DCSs over the scattering angle, product vibrational and rotational state distributions were also obtained.

Figure 2 presents the experimental 3D product contour plot of the DCSs at four different collision energies: 2.51, 3.97, 4.26, and 5.60 kJ/mol. The experimental DCSs show that H atom products are predominantly backward scattered relative to the HD beam direction in the CM frame. This phenomenon might be due to the greater contribution of small impact parameter. The angular distributions gradually become broader with the increase of the collision energies. Products from the DF ( $v'=1$ ) state only appear at the collision energy larger than 3.97 kJ/mol. The experimental result at 4.26 kJ/mol shows that the backward product peak of DF ( $v'=3$ ) is considerably higher than that of DF ( $v'=4$ ). This result is quite different from the previous experimental results [6]. Moreover, the vibrational branching ratio of the DF ( $v'=3$ ) product obtained here is also noticeably higher than that in Ref.[4]. Figure 3 shows the product vibrational state specific angular distribution at 5.60 kJ/mol, in good agreement with

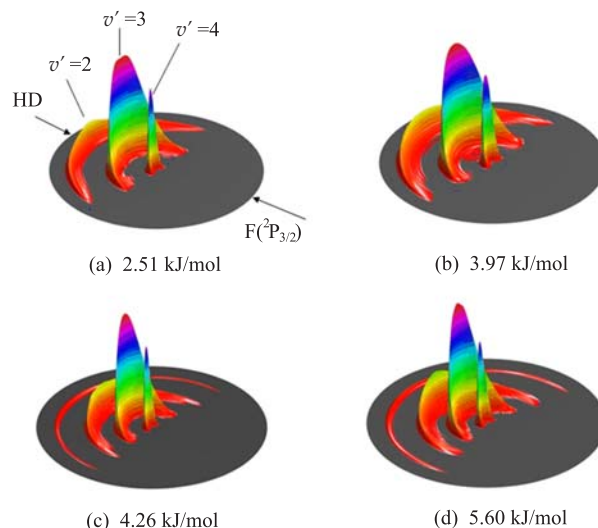


FIG. 2 The experimental three dimensional DCSs contour plots for the F+HD→DF+H reaction at four collision energies.

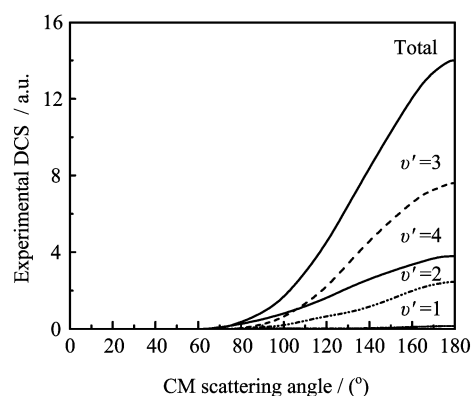


FIG. 3 The experimental DCS for the F+HD→DF+H reaction at 5.60 kJ/mol.

the theoretical results at 5.64 kJ/mol by Castillo and Manolopoulos [15].

### C. Product vibrational and rotational state distributions

Product vibrational branching ratios are determined exactly from the high resolution TOF spectra shown above. The DF vibrational state distributions from the F+HD reaction at eight different collision energies are presented in Fig.4, in which the sum of the vibrational branching ratios at each collision energy is set to be unity. Experimental results show that the vibrational branching ratio seems to be not dependent on the collision energy. In the collision energy studied, the DF ( $v'=3$ ) product is the most populated, about half of the products are populated on the  $v'=3$  state of DF. The branching ratio of the DF ( $v'=4$ ) state is about 40%, and displays a gradual decrease with the increase

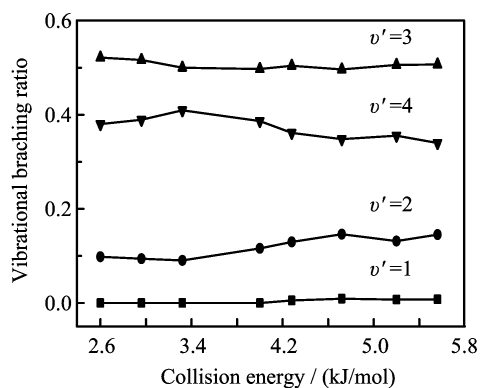


FIG. 4 Dependence of vibrational branching ratios on collision energy. Here, the sum of the vibrational branching ratios at each collision energy is set to be unity.

TABLE I Comparison of the experimental and the quantum-mechanical and quasi-classical trajectory vibration branching ratios for the reaction  $F+HD\rightarrow DF(v')+H$  at 5.60 kJ/mol.

	Vibration branching ratios			
	$v'=1$	$v'=2$	$v'=3$	$v'=4$
Theory (QM) [15]	0.015	0.149	0.485	0.351
Theory (QCT) [16]	–	0.130	0.413	0.457
Experiment (this work)	0.008	0.145	0.507	0.340

of the collision energy. And the branching ratio of the DF ( $v'=2$ ) state is around 10% and increase slightly with the increase of the collision energy. The branching ratios of the DF ( $v'=1$ ) state are zero till the collision energy is larger than about 4.18 kJ/mol. It is clear that the branching ratios of the four vibrational state show that  $DF(v'=3) > DF(v'=4) > DF(v'=2) > DF(v'=1)$  at the collision energy region studied in this work. Clearly, the DF vibrational state distribution is highly inverted. Table I shows a comparison between the DF vibrational branching ratios obtained at the collision energy of 5.60 kJ/mol with the results of both quantum mechanical (QM) [15] and quasiclassical trajectory (QCT) calculations [16]. The agreement between the experimental results of this work and the QM results is truly remarkable, while that between this work and the QCT results is not as good.

The excitation function for this reaction is also measured. In a single experiment, the backward scattering signals of the reaction were measured at different collision energies to determine the relative signals at different collision energies. The DCSs results were then calibrated with this relative ratio. The excitation function can then be determined by integrating the calibrated DCSs at different collision energies. The determined excitation functions of the four DF vibrational states and the total cross section are presented in Fig.5. It appears that the signal become too weak to be detected when the collision energy is lower than 2.51 kJ/mol. In

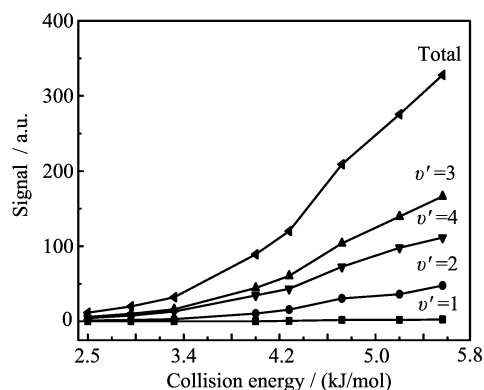


FIG. 5 Experimental excitation functions of the DF product at four vibrational states and the total excitation function of this reaction.

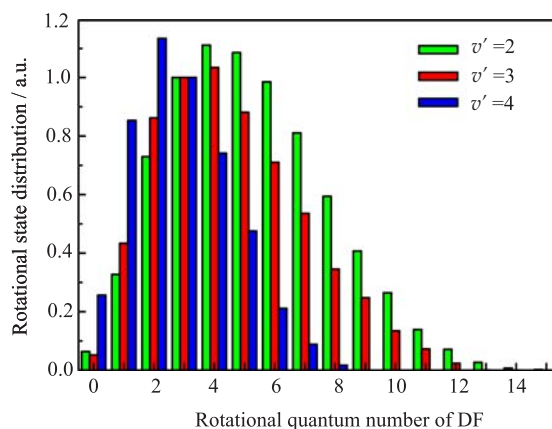


FIG. 6 The experimental rotational state distribution of the DF product at  $v'=2, 3$ , and  $4$  at the collision energy of 5.60 kJ/mol. The population of  $j=3$  state of each vibrational state is set to be equal.

contrast to the  $HF+D$  channel, no clear structures on the experimental excitation functions were observed for the  $DF+H$  channel. The excitation functions of all four DF vibrational state products behave similarly as the collision energy increase. This is not surprising since vibrational state branching ratios do not change much at differential collision energies.

Rotational state distributions for different vibrationally excited DF products were also determined. Figure 6 shows the rotational state distributions of the DF product at  $v'=2, 3$ , and  $4$ . To make the comparison clear, we set the population of  $j=3$  state of each vibrational state to be equal. The experimental results indicate that different DF vibrational state product has noticeably different rotational state distributions. It seems that at higher vibrational excitation of DF, the product rotational excitation is smaller. This is quite reasonable because the total available energy for the high  $v'$  DF product channel is less for partition into rotation and translation.

#### IV. CONCLUSION

We have investigated the dynamics of the F+HD→DF+H reaction channel at low collision energies using the high resolution H-atom Rydberg tagging technique. State-resolved DCSs were obtained at eight collision energies ranging from 2.51 kJ/mol to 5.60 kJ/mol. The DCSs show a predominantly backward scattering peak, and the peak becomes broader as the increase of the collision energy. Experimental excitation function rises monotonically as the collision energy increases. Product vibration branching ratio for each DF vibrational state product is nearly constant in the whole collision energies region studied. From the vibrational branching ratios, the DF vibrational distribution is highly inverted. Threshold of the products DF ( $v'=1$ ) was determined. Rotational state distributions for different DF vibrational state have been also determined. It seems that the rotational excitation is anti-correlated with the DF vibrational excitation. The DCS and product vibration branching ratio measured at 5.60 kJ/mol is in rather good agreement with the previous quantum dynamics calculations.

#### V. ACKNOWLEDGMENTS

This work was supported by the Chinese Academy of Sciences, the Ministry of Science and Technology, and the National Natural Science Foundation of China.

- [1] D. M. Neumark, A. M. Wodtke, G. N. Robinson, C. C. Hayden, K. Shobatake, R. K. Sparks, T. P. Schafer, and Y. T. Lee, *J. Chem. Phys.* **82**, 3067 (1985).
- [2] R. T. Skodje, D. Skouteris, D. E. Manolopoulos, S. H. Lee, F. Dong, and K. P. Liu, *Phys. Rev. Lett.* **85**, 1206 (2000).
- [3] R. T. Skodje, D. Skouteris, D. E. Manolopoulos, S. H. Lee, F. Dong, and K. Liu, *J. Chem. Phys.* **112**, 4536 (2000).
- [4] F. Dong, S. H. Lee, and K. Liu, *J. Chem. Phys.* **113**, 3633 (2000).
- [5] W. W. Harper, S. A. Nizkorodov, and D. J. Nesbitt, *J. Chem. Phys.* **116**, 5622 (2002).
- [6] F. Dong, S. H. Lee, and K. P. Liu, *J. Chem. Phys.* **124**, 8 (2006).
- [7] S. H. Lee, F. Dong, and K. P. Liu, *J. Chem. Phys.* **125**, 10 (2006).
- [8] Z. F. Ren, L. Che, M. H. Qiu, X. A. Wang, W. R. Dong, D. X. Dai, X. Y. Wang, X. M. Yang, Z. G. Sun, B. Fu, S. Y. Lee, X. Xu, and D. H. Zhang, *Proc. Natl. Acad. Sci. USA* **105**, 12662 (2008).
- [9] E. Rosenman, S. HochmanKowal, A. Persky, and M. Baer, *Chem. Phys. Lett.* **257**, 421 (1996).
- [10] D. H. Zhang, S. Y. Lee, and M. Baer, *J. Chem. Phys.* **112**, 9802 (2000).
- [11] T. X. Xie, Y. Zhang, M. Y. Zhao, and K. L. Han, *Phys. Chem. Chem. Phys.* **5**, 2034 (2003).
- [12] H. Kornweitz and A. Persky, *J. Phys. Chem. A* **108**, 8599 (2004).
- [13] T. Takayanagi, *Chem. Phys. Lett.* **433**, 15 (2006).
- [14] D. De Fazio, V. Aquilanti, S. Cavalli, A. Aguilar, and J. M. Lucas, *J. Chem. Phys.* **125**, 8 (2006).
- [15] J. F. Castillo and D. E. Manolopoulos, *J. Chem. Soc. Faraday Discuss.* **110**, 119 (1998).
- [16] F. J. Aoiz, L. Banares, V. J. Herrero, V. S. Rabanos, K. Stark, I. Tanarro, and H. J. Werner, *Chem. Phys. Lett.* **262**, 175 (1996).
- [17] F. J. Aoiz, L. Banares, V. J. Herrero, V. S. Rabanos, K. Stark, and H. J. Werner, *J. Chem. Phys.* **102**, 9248 (1995).
- [18] X. M. Yang and D. H. Zhang, *Acc. Chem. Res.* **41**, 981 (2008).
- [19] M. H. Qiu, Z. F. Ren, L. Che, D. X. Dai, S. A. Harich, X. Y. Wang, X. M. Yang, C. X. Xu, D. Q. Xie, M. Gustafsson, R. T. Skodje, Z. G. Sun, and D. H. Zhang, *Science* **311**, 1440 (2006).
- [20] L. Che, Z. F. Ren, X. G. Wang, W. R. Dong, D. X. Dai, X. Y. Wang, D. H. Zhang, X. M. Yang, L. S. Sheng, G. L. Li, H. J. Werner, F. Lique, and M. H. Alexander, *Science* **317**, 1061 (2007).
- [21] Z. F. Ren, L. Che, M. H. Qiu, X. G. Wang, D. X. Dai, S. A. Harich, X. Y. Wang, X. M. Yang, C. X. Xu, D. Q. Xie, Z. G. Sun, and D. H. Zhang, *J. Chem. Phys.* **125**, 151102 (2006).
- [22] X. G. Wang, W. R. Dong, M. H. Qiu, Z. F. Ren, L. Che, D. X. Dai, X. Y. Wang, X. M. Yang, Z. G. Sun, B. N. Fu, S. Y. Lee, X. Xu, and D. H. Zhang, *Proc. Natl. Acad. Sci. USA* **105**, 6227 (2008).
- [23] M. H. Qiu, Z. F. Ren, L. Che, D. X. Dai, S. A. Harich, X. Y. Wang, and X. M. Yang, *Chin. J. Chem. Phys.* **19**, 93 (2006).
- [24] L. Schnieder, W. Meier, K. H. Welge, M. N. R. Ashfold, and C. M. Western, *J. Chem. Phys.* **92**, 7027 (1990).
- [25] L. Schnieder, K. SeekampRahn, E. Wrede, and K. H. Welge, *J. Chem. Phys.* **107**, 6175 (1997).
- [26] Z. F. Ren, M. H. Qiu, L. Che, D. X. Dai, X. Y. Wang, and X. M. Yang, *Rev. Sci. Instrum.* **77**, 016102 (2006).
- [27] M. H. Qiu, L. Che, Z. F. Ren, D. X. Dai, X. Y. Wang, and X. M. Yang, *Rev. Sci. Instrum.* **76**, 083107 (2005).